Carbohydrate Research, 229 (1992) 41–55
Elsevier Science Publishers B.V., Amsterdam

Molecular and crystal structure of konjac glucomannan in the mannan II polymorphic form*

Toshifumi Yui[1], Kozo Ogawa[2] and Anatole Sarko

Chemistry Department, State University of New York, College of Environmental Science and Forestry, Syracuse, NY 13210 (USA)

(Received June 20th, 1991; accepted November 15th, 1991)

ABSTRACT

A probable crystal structure of konjac glucomannan (mannose:glucose ratio = 1.6) is proposed based on X-ray data and constrained linked-atom least-squares model refinement. The structure crystallizes in the mannan II polymorphic form, in an orthorhombic unit-cell with $a = 9.01$ Å, $b = 16.73$ Å, c (fiber axis) = 10.40 Å, and a probable space group $I222$. The backbone conformation of the chain is a two-fold helix stabilized by intramolecular O-3–O-5′ hydrogen bonds, with the O-6 rotational position *gt*. The unit cell contains four chains with antiparallel packing polarity and eight water molecules which reside in crystallographic positions. Intermolecular hydrogen bonds occur exclusively between chains and water molecules, establishing a three-dimensional hydrogen-bond network in the crystal structure. The glucose residues replace mannoses in the structure in isomorphous fashion, although some disorder appears possible. A structure having alternating $gg - gt$ O-6 rotational positions and conforming to space group $P222$ appears to describe the disorder regions of the crystal. The reliability of the structure analysis is indicated by the X-ray residuals $R = 0.276$ and $R'' = 0.223$.

INTRODUCTION

Mannans constitute an abundant and diverse group of polysaccharides in which the chain-backbone sugar units are predominantly D-mannose. Although mannans of several different linkage-types are known, the β-(1→4)-linked mannans, such as occurring as major constituents of the endosperms of palm[1], date[2], coffee bean[4], and ivory nuts[1], as well as the cell walls of several green and some red algae[4–7], are widely distributed in nature. Sequences of β-(1→4)-linked D-mannose are also present in the linear copolymer glucomannan, and the branched copolymers

Correspondence to: Dr. A. Sarko, Chemistry Department, State University of New York, Collgege of Environmental Science and Forestry, Syracuse, NY 13210, USA.

* Part 18 in the series Packing Analysis of Carbohydrates and Polysaccharides.

[1] Faculty of Engineering, Miyazaki University, Miyazaki 889-4, Japan.

[2] Research Institute for Advanced Science and Technology, University of Osaka Prefecture, Osaka 593, Japan.

galactomannan. Glucomannans, in which the β-D-glucosyl residues are interspersed between mannosyl residues in an apparently random fashion, are found in hemicelluloses of several softwoods[8] and the bulbs and the endosperm of various plants such as *Amorphophallus konjac*, the material used in the present study.

Pure β-(1→4)-mannans are, to an extent, similar to cellulose in that both exist as a crystalline structural component of cell walls. However, mannans differ from cellulose in that their physical state is not uniform, even within one species[4]. It has also been reported that mannan has a considerably lower molecular weight and that its microfibrils are much more sensitive to physical and chemical treatment than are those of cellulose[9].

The ultrastructure and crystalline morphology of cell-wall mannans have been subject to some study by electron microscopy and X-ray diffraction techniques. Frei and Preston were the first to report a thorough investigation of the architecture of mannan cell walls in the siphoneus green algae[4]. No sign of microfibrils similar to those in cellulosic cell-walls was detected by electron microscopy; instead, the surface of the wall was found to be granular or to have short rodlet-like structures. It was also shown, by X-ray diffraction studies, that the mannan chains were arranged transversely in the outer layers of the algae, whereas they tended to lie longitudinally in the inner layers. In the same study, the first, well-oriented X-ray fiber diagram of mannan was obtained from the inner layers. When the cell-wall materials were treated with alkali solutions, a different X-ray diagram was obtained. These materials were moisture sensitive and were, therefore, thought to be hydrated polymorphic forms. The native and the alkali-treated polymorphs were named mannan I and mannan II, respectively, by analogy with the well-known cellulose I and cellulose II polymorphs. A two-fold chain conformation, another feature akin to cellulose, was also apparent in both polymorphs, with a similar fiber repeat to that of celluloses.

Prior to Frei and Preston's work, mirofibrils of mannan had been observed in the cell walls of the ivory nut endosperm and date seeds[2]. These mannans occurred in two forms termed A and B, differing in molecular weight, and, whereas mannan A appeared granular in the electron microscope, mannan B with the higher molecular weight appeared microfibrillar in texture. Similarly, in the case of the algal mannan, cautious treatment of the cell walls under mild extraction conditions allowed observation of microfibrillar regions in addition to the dominant granular ones in the electron microscope[9]. It was, therefore, concluded that mannan was present in the walls in two types: a granular and a microfibrillar form, and that these two forms probably had different regional distributions.

Additional examination by electron diffraction of the cell-wall mannan from green algae and ivory nuts demonstrated that alkali-resistant microfibrillar components corresponded to mannan II, whereas alkali-soluble granular components consisted of mannan I[10]. This was surprising in comparison with cellulose, since for the latter only one native polymorph — cellulose I — is known. A possible interpretation of these results suggested that the granular components of mannan I

served as the cementing or encrusting substance, similar to hemicellulose in cellulosic walls, while the mannan II microfibrils corresponded to skeletal cellulose ones.

It was further shown through studies of the recrystallization behavior of both ivory nut mannan[10–12] and glucomannans from various origins[13] that the formation of single crystals of either mannan I or mannan II depended on three factors: the temperature of crystallization, the polarity of the crystallization medium, and the chain length of the polysaccharide. High temperature, low polarity, and low chain length favored the formation of mannan I, whereas low temperature, high polarity, and high chain length yielded the mannan II polymorph.

Single crystals of mannan I gave a granular precipitate consisting of lozenge-shaped lamellae in which the chain axes of the molecules were oriented perpendicular to the lamellar plane. On the other hand, in mannan II, small square crystals were laterally connected as blocks on a string to form a pseudo-fibrillar precipitate, and in no case was the chain axis perpendicular to the large crystal plane[11,13].

In one study of glucomannans[13] it was suggested that isomorphous replacement of mannose by glucose occurred in the crystal structure. All glucomannan samples that were examined did not only crystallize into the mannan type lattices, but also their base-plane unit cell dimensions revealed a degree of constancy. No correlation could be established between the variation of the base-plane parameters and the glucose content. Only the perfection of crystals was found to be diminished in specimens having a high glucose content.

Several attempts to solve the detailed crystal structure have been made, mainly for the mannan I polymorph which was, at first, believed to be the only native form. The earlier attempts to analyze the X-ray diffraction data obtained from the cell walls of algae encountered difficulties because the analysis of the data was complicated by the presence of additional phases and other impurities in the specimens[4,14]. More recently, however, Chanzy and coworkers have proposed a reasonable crystal and molecular structure[15] of mannan I, based on electron diffraction data collected from mannan I single crystals. An important conclusion reached from this study was the existence of two-fold screw axes parallel to both *a* and *b* unit cell dimensions which definitely eliminated parallel chain packing for mannan I.

The only previous attempt to determine the crystal structure of mannan II was made by Okuyama and coworkers[16], by analyzing the original Frei and Preston mannan II data from the green algae[4]. The principal features proposed for this mannan II model were a four-chain unit cell with antiparallel chain packing and containing eight water molecules. Because of the qualitative nature of the Frei–Preston data, however, a complete structure analysis could not be completed. The present investigation of the *Amorphophallus konjac* glucomannan was, therefore, undertaken with two objectives in mind: (*1*) to examine the Okuyama mannan II model with the help of the glucomannan data, and (*2*) and more importantly, to try to determine the structural characteristics of the glucomannan copolymer. The

konjac glucomannan (KGM) has the highest[17] molecular weight (dp = 6000) and the highest[18] glucose content (mannose/glucose ratio = 1.6) among all glucomannan samples whose crystallization behavior has been studied[13]. These properties of KGM apparently cause it to crystallize persistently in the mannan II polymorphic form, regardless of crystallization conditions[13]. In addition to refining Okuyama's model, other possible packing structures with different space groups were also to be tested.

EXPERIMENTAL

Sample preparation.—The purified KGM that had been extracted from *Amorphophallus konjac* flour was supplied by Dr. T. Mizuno of Sizuoka University in the form of the acetyl derivative. The acetylated sample (KGM-Ac) was cast as a clear film from $CHCl_3$ solution. Strips of the film were stretched in glycerine at 155° up to five times the original length. The stretched films were deacetylated in 2 M methanolic NaOMe overnight at room temperature, while keeping the samples at constant length.

The density of the samples was measured by flotation in a mixture of *o*-xylene and $CHCl_3$.

X-ray diffraction measurements.—The X-ray fiber patterns were recorded in a flat-film camera with Ni-filtered Cu$K\alpha$ radiation, under high relative humidity in a helium atmosphere.

Relative intensities of the diffraction peaks were obtained from radial tracings recorded with a Joyce–Loebl Mark IIIc microdensitometer. The areas under the tracings were resolved (as far as possible) into individual intensities with a least-squares curve resolution program[19] and subsequently corrected[20] for Lorentz and polarization factors[21], a temperature factor[22], and arcing of the reflections. The square roots of the corrected intensities constituted the relative, observed structure-factor amplitudes. Unobserved reflections were assigned relative intensities of one-half of the minimum observable value in the corresponding region of the diffraction angle.

Structure determination and refinement.—Model building and structure refinement were carried out using the constrained linked-atom least-squares refinement program LALS[23,24]. The program seeks to minimize the function defined by the relation:

$$\Omega = \sum_m w_m \mid F_{om} - F_{cm} \mid^2 + S\sum_{ij} \epsilon_{ij} + \sum_q \lambda_q G_q \qquad (1)$$

In this equation, the first term ensures optimum agreement between the observed (F_{om}) and calculated (F_{cm}) structure factor amplitudes of m independent reflections. The weights, w_m, for individual reflections were assigned a value of 1.0 for all observed reflections, 0.5 for unobserved reflections when $F_{om} < F_{cm}$ or 0 when $F_{cm} < F_{om}$.

The second term in eq *1* minimizes nonbonded interactions arising in the structure. The quantity ϵ_{ij} is defined by a quadratic expression

$$\begin{aligned} \epsilon_{ij} &= w_{ij}\left(d_{ij} - d_{ij}^0\right)^2 \quad \text{when } d_{ij} < d_{ij}^0 \\ &= 0 \qquad\qquad\qquad\quad \text{when } d_{ij} > d_{ij}^0 \end{aligned} \tag{2}$$

where d_{ij} is the nonbonded distance between atoms i and j in the model, d_{ij}^0 is the cutoff distance for the same atom pair, and w_{ij} is the weight for this interaction.

The final term of eq *1* imposes, by the method of undetermined Lagrange multipliers λ_q, the constraints of a set of coordinate equations, G_q, which are used to ensure helix continuity and ring closure in the sugar residue.

RESULTS AND DISCUSSION

X-Ray diffraction data.—Fig. 1 shows a typical X-ray diffraction pattern of KGM, recorded under high relative humidity conditions. The latter produced higher crystallinity and greater spot sharpness, suggesting a hydrated form of the structure. Table I lists the observed *d* spacings of the reflections, along with their visually estimated intensities. Also shown, for comparison, are the data for the algal mannan II of Frei and Preston[4]. Good agreement between the two data sets,

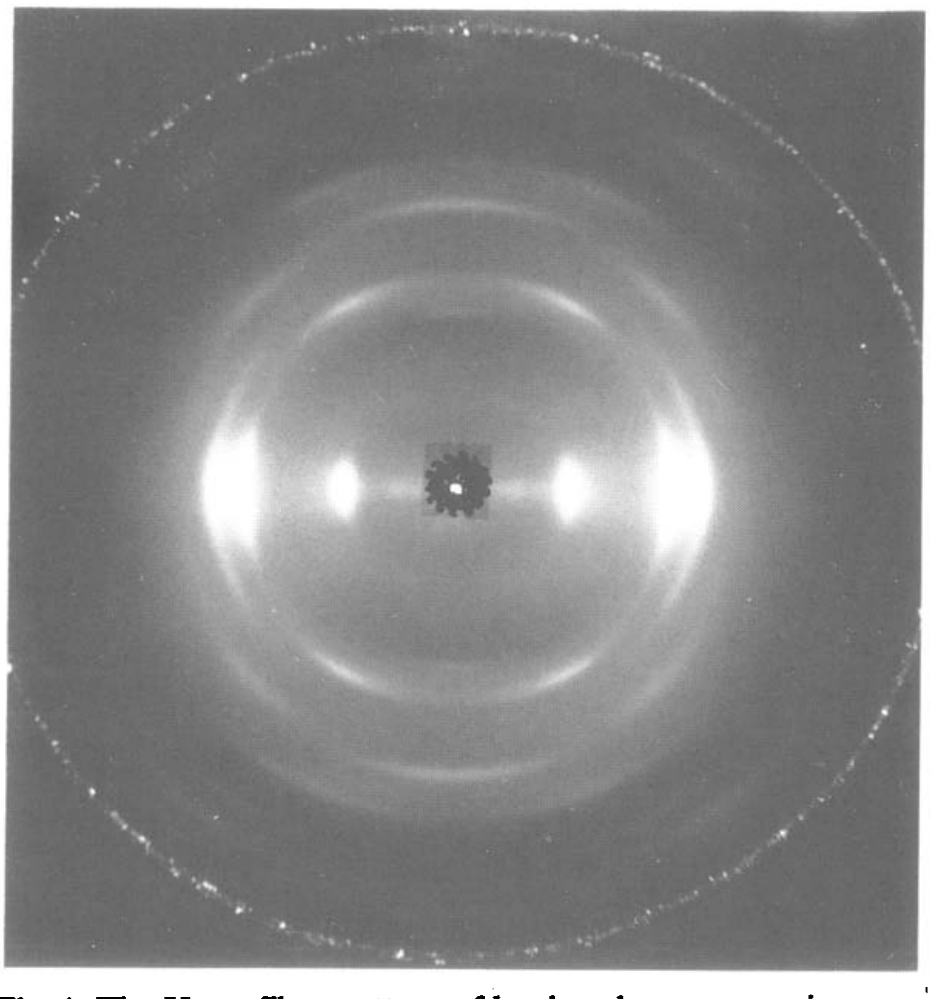

Fig. 1. The X-ray fiber pattern of konjac glucomannan in mannan II polymorphic form. The fiber axis is vertical.

TABLE I

Comparison of calculated and observed d spacings, and observed intensities for konjac glucomannan and algal mannan in mannan II polymorphic form (Å)

hkl	d_{calcd}	Konjac glucomannan		Algal mannan	
		d_{obsd}	I^a_{obsd}	d_{obsd}	I^a_{obsd}
020	8.362	8.280	vs	8.26	vs
200	4.507	4.530	vs	4.50	vs
220	3.967	3.967	vs	3.95	vs
310	2.957			2.95	vw
060	2.787			2.74	vwd
160	2.663			2.67	vwd
340	2.440			2.47	vwd
260	2.371			2.35	vwd
410	2.233	2.234	w	2.26	w
011	8.831	8.935	vvw	8.73	w
211	4.014	4.015	m	3.99	m
141	3.563	3.577	vw	3.57	w
321	2.729	2.714	vvw	2.74	w
331	2.563	2.568	vvw	2.59	w
071	2.329			2.35	wd
002	5.199	5.218	w	5.10	s
012	4.965	4.867	vvw	4.70	w
022	4.415	4.397	s	4.29	s
132	3.503	3.505	m	3.48	ms
152	2.685	2.691	vvw	2.73	w
062	2.457			2.47	vw
013	3.394	3.405	m	3.35	s
123	3.017	3.028	m	3.02	w
213	2.711	2.708	w	2.69	w
143	2.559	2.562	w	2.55	mw
233	2.464	2.447	vvw	2.47	w
333	2.103	2.10	vw	2.10	wd
004	2.599	2.594	w	2.55	vw
014	2.569			2.53	vvw
024	2.482	2.484	w	2.45	w
204	2.252	2.259	w	2.25	w
224	2.174	2.173	vw	2.16	w
154	2.001			1.99	vw

[a] Abbreviations: vs, very strong; s, strong; ms, medium strong; m, medium; w, weak; vw, very weak; vvw, very very weak; d, diffuse.

both in d spacings and intensity patterns, is indicative of considerable similarity between the mannan II polymorph and KGM. However, several reflections observed in the algal mannan, particularly those with very weak intensities on the equator, are apparently missing in the KGM data. The fact that KGM is a highly pure material, while the algal mannan may be heterogeneous, suggests that spurious additional reflections other than those originating from true mannan II may be present in the original data set.

The refinement of the unit-cell parameters resulted in an orthorhombic unit cell with dimensions $a = 9.01$ Å, $b = 16.73$ Å, and c (fiber axis) $= 10.40$ Å. (The

observed and calculated d spacings are compared in Table I.) Based on the unit cell contents of four mannobiose units and eight water molecules, the calculated density of 1.525 g/cm^3 is in good agreement with the experimental value of 1.507 g/cm^3. A substantially identical unit cell for mannan II was proposed by Okuyama et al. ($a = 8.99$ Å, $b = 16.54$ Å, and $c = 10.36$ Å) who also suggested the $I222$ space group for the structure[16]. This space group demands $(h + k + l) = odd$ reflections to be absent, i.e., the extinction rule of a body-centered lattice symmetry. In the KGM case, the indexing of all reflections, except the (*012*) reflection on the second layer line, were in accord with the extinction rule. Since the latter reflection is very faint with negligible intensity, the crystal-structure analysis of the KGM-mannan II was initially carried out in $I222$ space group, eliminating the (*012*) reflection from the X-ray data set. As described below, other space groups were examined later during the course of refinement, in an attempt to account for this reflection.

Structure analysis of the I*222 models.*—A conformational model of the mannan chain with a two-fold screw symmetry and a repeat of 10.40 Å was generated by minimizing the nonbonded interactions (the 2nd term of eq *1*) within the isolated chain. As had been suggested by the energy calculations of the chain[25,26] and the structure analysis[14,15] of mannan I, an intramolecular hydrogen bond between O-3–O-5′ atoms across the 1→4 linkage was introduced into the model. The conformational parameters which were allowed to vary during this analysis are illustrated in Fig. 2, namely, the conformation angles ϕ and ψ at the glycosidic linkage, the bridge angle of the linkage, τ, and the rotation angle of O-6 atoms, χ. Three initial conformational models were established on the basis of staggered positions of the O-6 atom: *gg*, *gt*, and *tg*[27].

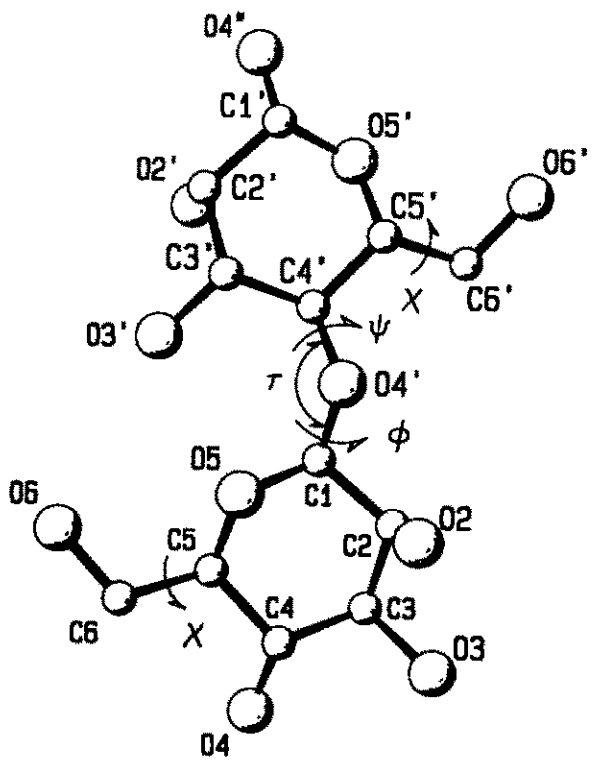

Fig. 2. The atomic labeling scheme and designation of the conformational parameters ϕ, ψ, χ, and τ.

These chain models, along with water molecules, were placed in the unit cell with helix axes of the chains parallel to the c axis of the unit cell, and their best packing positions were obtained by minimizing eq *1*. The symmetry requirements of the $I222$ space group defined completely the base plane positions of the first helix axis and two independent water molecules. The remaining three chains and six water molecules were generated by symmetry operations. Therefore, the parameters to be refined in the molecular-packing analysis were the translations along c for the chain, w, and for the two waters, w_1 and w_2, as well as the chain rotation about the helix axis, μ. For the X-ray data, a scaling factor, K, and an attenuation factor, A, were also refined.

The packing models thus obtained were subjected to the simultaneous adjustment of chain-conformation and molecular-packing parameters. During this stage of analysis, intermolecular hydrogen bonds were introduced whenever appropriate oxygen atoms were found to be within 1.8–3.2 Å distance. Due to a relatively loose packing in this structure, which is typical of hydrate crystal structures, the hydrogen bond attractions were the dominant intermolecular interactions, compared with nonbonded repulsions.

The next step in the structure analysis was to examine the effect of a glucose residue isomorphously replacing a mannose in the KGM-mannan II structure. For practical reasons, this was achieved by constructing a residue in which the O-2 atom occupied equatorial and axial orientations with varying occupancies. A given ratio of axial/equatorial O-2 atoms in the residue, each contributing appropriately to atomic interactions and the atomic scattering factors, thus represented a desired mannose/glucose ratio (M/G ratio) in the crystal structure.

A series of one-cycle refinements were carried out with various M/G ratios to determine its most probable value. The results are shown in Fig. 3, separately for each of the three O-6 models. As is obvious from these results, the O-6-*gt* and *tg* models, showing similar behavior in the R''-factors, indicate a minimum in the latter around 70–80% mannose content (M/G ratio 2.3–4.0). In the O-6-*gg* model, the R''-factor continues to decrease with the decreasing mannose content, reaching a minimum at 30% mannose. The latter figure, which is indicative of a glucose-rich molecule, is not a reasonable result. It is clear, however, that the X-ray residuals show distinct improvement after introducing the glucose O-2 atoms.

A few runs of the structure refinement were made to provide the final models of KGM-mannan II as described by the hybrid residue. The values of the M/G ratio corresponding to the minima shown in Fig. 3 were assigned appropriately to the O-6-*gt* and *tg* models, while for the O-6-*gg* model, the chemically defined ratio M/G = 1.6, was arbitrarily assigned. Table II lists the X-ray residuals, hydrogen bonds, and short contacts resulting from these refinements. It should be noted that the general packing features of both the chains and the water molecules were found to be very similar in the three models, with the only structural differences arising mainly from different O-6 rotational positions and the consequent hydro-

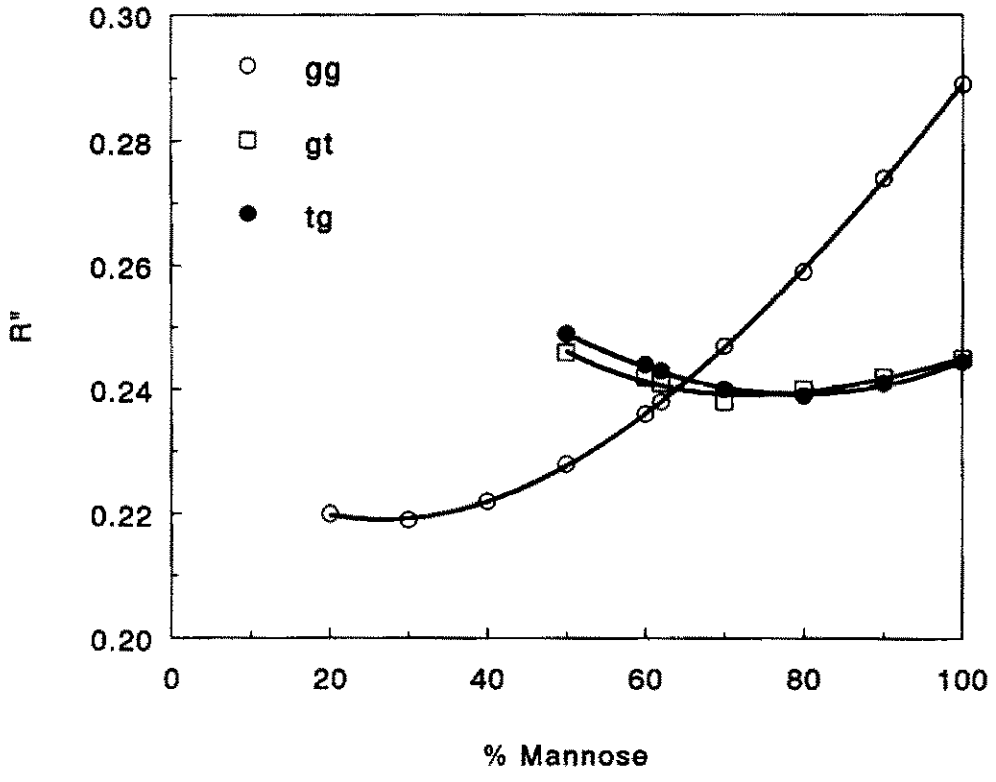

Fig. 3. Variation of the R''-factor of $I222$ models with varying mannose content.

gen-bond schemes. For example, inspection of the O-6-*tg* model revealed the presence of severe short contacts between the O-6 atoms of neighboring chains. It was also found that the hydrogen-bonding scheme of this model was improbable because of a concentration of bonds to the W2 water molecule while leaving the W1 water molecule unbonded. On the other hand, the hydrogen bonds formed in the O-6-*gg* and *gt* models were much more probable, with every water molecule and all hydroxyl oxygens (that is, O-2, O-3, and O-6) participating in hydrogen bonding. For example, one of the O-6 atoms in the O-6-*gg* model could participate in three hydrogen bonds which linked two other O-6 atoms and the W1 water molecule. The hydrogen bonds of the O-6-*gt* model were the most probable, consisting mostly of strong water-chain interactions. All water molecules occupied the centers of four symmetric bonds to surrounding chains. Such a scheme of bonds appeared to provide the best three-dimensional stabilization of the structure, utilizing water molecules efficiently.

Since no significant differences in the R- and R''-factors were evident among the three models, the structural advantages of the O-6-*gt* model, as provided by its hydrogen-bonding scheme, was taken as indicative of its higher probability to represent the KGM-mannan II structure. The final values of the refined parameters for this model are summarized in Table III and its atomic coordinates are given in Table IV. Two projections of the unit cell, complete with hydrogen bonds, are shown in Fig. 4. A comparison of the calculated and observed structure factor amplitudes is given in Table V, showing generally good agreement.

Disorder in the crystal structure.—The presence of the faint (*012*) reflection raised the question of possible disorder in the structure of KGM-mannan II, occurring as a deviation from $I222$ symmetry. This reflection did not occur only in

TABLE II

Hydrogen bonds and short contacts of the final four models

Contact type	Atoms[a]	Contact distance (Å)	No. of contacts per unit cell
1. *I*222 O-6-*gg* model: M/G = 1.6 $R = 0.289$ $R'' = 0.222$			
H-bonds:	$O\text{-}6_1$–$O\text{-}6_2$	2.95	4
	$O\text{-}6_1$–$O\text{-}6_4$	2.86	4
	$O\text{-}2_1$–$O\text{-}3_4$	2.92	4
	$O\text{-}6_1$–$W1'_4$	2.80	8
	$O\text{-}2_1$–$W2'_1$	2.89	8
contacts:	$H\text{-}6a_1$–$W2_4$	2.19	8
2. *I*222 O-6-*gt* model: M/G = 0.7/0.3 $R = 0.276$ $R'' = 0.223$			
H-bonds:	$O\text{-}3_1$–$W1_4$	3.09	8
	$O\text{-}6_1$–$W1'_4$	2.83	8
	$O\text{-}6_1$–$W2_4$	2.76	8
	$O\text{-}2_1$–$W2'_1$	2.78	8
contacts:	$H\text{-}3_1$–$H\text{-}3_4$	1.93	4
	$H\text{-}6b_1$–$H\text{-}6b_4$	1.86	4
3. *I*222 O-6-*tg* model: M/G = 0.8/0.2 $R = 0.308$ $R'' = 0.235$			
H-bonds:	$O\text{-}6_1$–$O\text{-}6_3$	2.05	4
	$O\text{-}6_1$–$W2_4$	2.83	8
	$O\text{-}2_1$–$W2'_1$	2.92	8
contacts:	$O\text{-}6_1$–$O\text{-}6_3$	2.05	4
	$H\text{-}5_1$–$O\text{-}2'_4$	2.13	8
4. *P*222 O-6-*gg*, O-6′-*gt* model: M/G = 1.6 $R = 0.237$ $R'' = 0.190$			
H-bonds:	$O\text{-}6_1$–$O\text{-}6_2$	2.81	2
	$O\text{-}6_1$–$O\text{-}6_4$	2.86	2
	$O\text{-}6_1$–$W2_3$	2.84	4
	$O\text{-}2_1$–$W3_1$	2.88	4
	$O\text{-}6'_1$–$W1_4$	2.77	4
	$O\text{-}6'_1$–$W3_4$	2.74	4
	$O\text{-}2'_1$–$W4_1$	2.73	4
	$W1_1$–$W1_4$	2.74	1
	$W2_1$–$W2_3$	2.86	1
contacts:	$H\text{-}6a_1$–$W4_3$	2.15	4

[a] Subscripted symmetry codes indicate the following equivalent positions: 1: x, y, z; 2: $-x, -y, z$; 3: $x, -y, -z$; 4: $-x, y, -z$. The translational positions of chains are (1/4, 1/4, w) for both *I*222 and *P*222. Translational positions for water molecules are: For *I*222, W1: $(0, 1/2, w_1)$; W1′: $(1/2, 0, 1/2+w_1)$; W2: $(0, 0, w_2)$; W2′: $(1/2, 1/2, 1/2+w_2)$. For *P*222, W1: $(0, 1/2, w_1)$; W2: $(1/2, 0, w_2)$; W3: $(1/2, 1/2, w_3)$; W4: $(0, 0, w_4)$. Note that: $R = \Sigma \| F_o | - | F_c \| / \Sigma | F_o |$; $R'' = [\Sigma w \| F_o | - | F_c \|^2 / \Sigma | F_o |^2]^{1/2}$.

KGM-mannan II, it has also been observed in mannan II data from green algae[4] (see Table I). A slight, but probable, structural change to allow this reflection to occur is to decrease the *I*222 symmetry to that of *P*222, which is achieved by removing a two-fold screw constraint from the chain conformation and allowing four water molecules to be independent. The first condition also allows the residues of a given chain to have independent O-6 dispositions within the manno-biose unit, thus yielding an additional three models with alternating, mixed O-6

TABLE III

Summary of the final parameter values for the *I*222 O-6-*gt* model

Parameter	Value	Comments
Conformational parameters		
χ	57.42°	torsion angle of O-5–C-5–C-6–O-6[a]
ϕ	23.54°	torsion angle of H-1–C-1–O-1–C-4′[a]
ψ	−25.15°	torsion angle of C-1–O-1–C-4′–H-4′[a]
τ	115.60°	bond angle of C-1–O-1–C-4′
Packing parameters		
μ	−128.19°	chain rotation[b]
w, fractional	−0.101	c translation of chain
w_1, fractional	0.118	c translation of W1 water
w_2, fractional	−0.214	c translation of W2 water
Scaling parameters[c]		
K	7.818	scaling factor for F_o
A, Å^2	6.576	attenuation factor for F_c

[a] Conformation angle is 0° when the bond sequence is *cis*. Positive angle is for the far bond clockwise relative to the near bond. [b] 0° position is when O-4 is at 0, y, for a helix at the origin. Positive rotation is clockwise looking down the helix axis. [c] These parameters are used in the second term of the eq *1* in the form: $[KF_o - F_c\exp(-A\rho^2/4)]$ where ρ is a reciprocal-space radius for the reflection. (Note: For hydrogen bonds and short contacts, see model 2 in Table II.)

positions, that is *gg-gt*, *gg-tg*, and *tg-gt*. The structural refinement of the latter three *P*222 models was carried out using similar procedures as for the I222 models. The resulting structures indicated that the same structural features arising from the O-6 positions as were found in the *I*222 models were nearly preserved in the affected part of the unit cell. Especially, the undesirable features connected with the *tg* disposition of the O-6 atom still existed in the O-6-*gg-tg* and *tg-gt* models with short contacts between the O-6-*tg* atoms and the isolation of one of the four independent water molecules from hydrogen bond formation. Only the mixed O-6-*gg-gt* model formed an acceptable structure having no significant short contacts and fairly well distributed hydrogen bonds. The characteristics of this model are also shown in Table II. It should be noted that the lower values of the X-ray residuals for this model, as compared with those of the *I*222 models, may in part be attributable to an increased number of refinable parameters allowed by the *P*222 symmetry.

The space groups $P2_12_12_1$ and $P2_12_12$ were also tested to investigate the possibilities of packing structures other than those of the *I*222 and *P*222 types. Several models with $P2_12_12_1$ symmetry were quickly eliminated in the initial stages of refinement because of high *R*-values and serious mismatches of the observed and calculated structure-factor amplitudes, particularly for the reflections on higher order layer lines. On the other hand, the structure analysis of $P2_12_12$

TABLE IV

Fractional atomic coordinates of the final structure

Atom	x	y	z
C-1	0.23790	0.27030	0.28457
C-2	0.26155	0.33827	0.18929
C-3	0.20008	0.31600	0.05786
C-4	0.26409	0.23632	0.01374
C-5	0.24225	0.17305	0.11764
C-6	0.31482	0.09412	0.08409
O-6	0.29610	0.03645	0.18391
O-5	0.30688	0.19940	0.23654
O-1	0.30844	0.29004	0.39901
O-2[a]	0.41597	0.35471	0.17890
O-3	0.23678	0.37694	−0.03307
O-4	0.19156	0.20996	−0.10099
H-1	0.11832	0.25971	0.29700
H-2[a]	0.20805	0.39286	0.22578
H-3	0.07848	0.31156	0.06324
H-4	0.38322	0.24331	−0.00628
H-5	0.12296	0.16221	0.13157
H-6a	0.26493	0.07017	−0.00443
H-6b	0.43440	0.10335	0.06907
W1	0	0.5	0.11813
W2	0	0	−0.21423

[a] For the glucose residue, O-2: (0.19216, 0.40874, 0.23688); H-2: (0.38101, 0.35010, 0.17912).

models was continued until nine additional models with mixed O-6 positions were refined. (Unlike the $P222$ case, the structure of O-6-*gg*-*gt* was not equivalent to that of O-6-gt-gg and so on, due to the nature of $P2_12_12$ symmetry.) All final models showed reasonable X-ray residuals in the range $R = 0.250–0.313$ and $R'' = 0.207–0.238$. However, the resulting hydrogen bonding schemes of these $P2_12_12$ models, even with equal O-6 positions, were more complicated, less symmetrical, and generally inferior to those found in the $I222$ and $P222$ models. It was concluded that such models were not probable for the structure of KGM-mannan II.

CONCLUSIONS

As indicated by the analysis described here, the structure conforming to the $I222$ symmetry and with all O-6 atoms in the *gt* position appears to be the most probable average structure for KGM-mannan II. At the same time, it is very likely that some O-6 atoms may be in the *gg* position, which results in few disadvantages. Likewise, the above two features may combine in a mixed O-6-*gg*-*gt* model conforming to $P222$ symmetry whose likelihood is indicated by the presence of the (*012*) reflection — the only violator of the extinction rule of $I222$ symmetry. The very weak intensity of this reflection suggests only local and minor distortions of

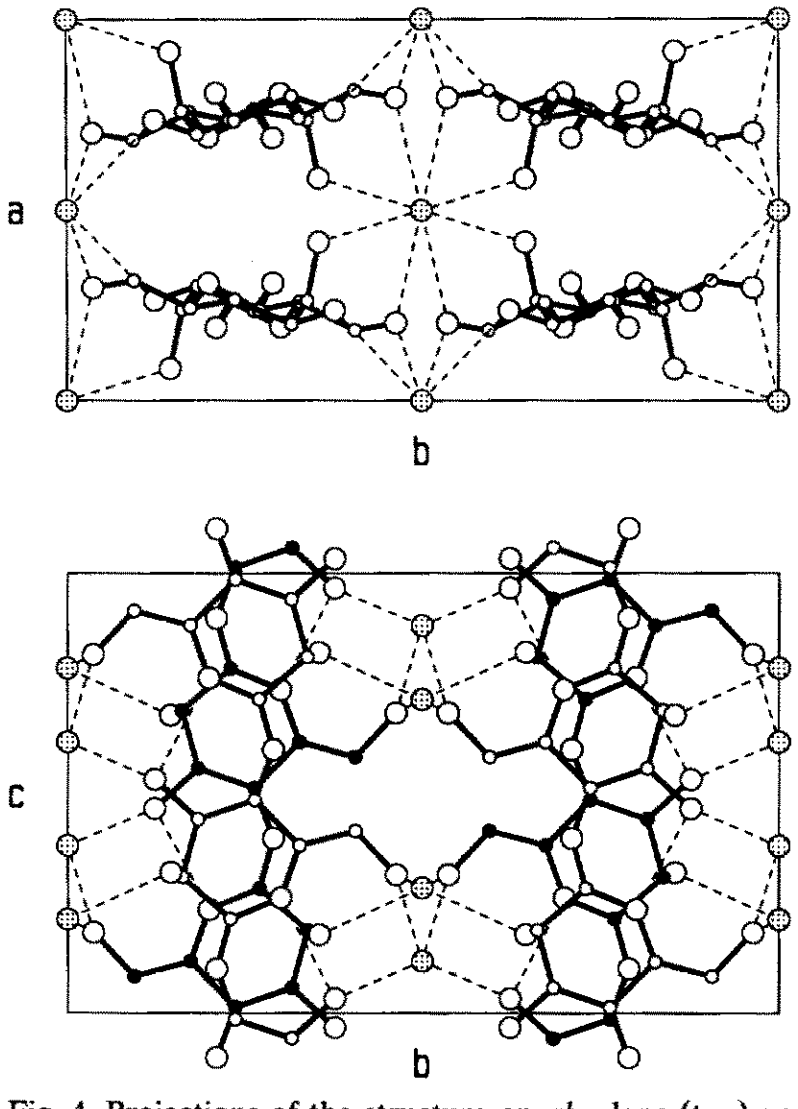

Fig. 4. Projections of the structure on *ab* plane (top) and *bc* plane (bottom). All hydrogen atoms have been omitted and hydrogen bonds are shown as dashed lines.

the *I*222 symmetry. Therefore, it is concluded that the crystal structure of KGM-mannan II is for the most part based on *I*222 O-6-*gt* regions, with occasional contributions from the *P*222 O-6-*gg*-*gt* structure which is readily derived from the former by an alternating arrangement of O-6 positions. It should be noted that the O-6-*gt* position is found[14,15] in both mannan I and mannotriose[26], whereas alternating *gg* and *gt* disposition of O-6 atoms have been found in mannobiose[28]. Recent solid-state ^{13}C-NMR spectroscopy of both mannan I and mannan II also indicates a preference for O-6-*gt* in both polymorphs[29].

The chemical structure of KGM has previously been determined by hydrolysis and methylation analysis using both acid hydrolysis[18] and enzymic hydrolysis with cellulase[30] and mannanase[31–33]. The general conclusion based on these studies was that the mannose sequences of the chain are at most pentameric in length and that these short segments are connected with only glucose or cellobiose units. It was also suggested that branching may occur approximately every 10–13 repeating units through a β-(1 → 3) linkage[34,35]. In view of this type of chemical structure of KGM, such chains would be thought rather unlikely to crystallize or, at best, would yield poor diffraction data. In fact, the X-ray diffraction data of KGM-triacetate show a high degree of disorder along the fiber axis[36] (which may also be due to

TABLE V

Comparison of calculated and observed structure-factor amplitudes

hkl	F_{calcd}	F_{obsd}	*hkl*	F_{calcd}	F_{obsd}
020	129.06	119.61	022,112	88.33	75.13
110	38.84	13.45[a]	132	77.58	106.32
130	26.60	21.26[a]	202	18.78	23.84[a]
200	266.10	265.03	042	43.88	25.80[a]
040	36.74	24.16[a]	222	26.71	27.36[a]
220	214.07	241.57	152	32.66	30.10
150	1.53	33.85[a]	013	39.30	29.47
240	35.20	34.87[a]	103	5.13	11.49[a]
310	78.60	21.11[a]	123	49.93	57.23
060	48.72	22.98[a]	033	7.07	12.12[a]
330	4.03	24.86[a]	213	56.16	37.14
260	35.83	29.71[a]	143	67.35	96.16
170	28.18	31.12[a]	233	24.99	38.46
400,350	87.18	81.31	053	20.79	22.28[a]
			303	31.76	25.64[a]
011	1.48	9.46	323	36.76	28.07[a]
101	21.38	10.79[a]	253	17.95	30.41[a]
121	11.91	15.79[a]	163	65.21	62.39
031	16.63	17.51[a]	024,114	38.23	25.80
211	81.29	97.72	134,204	64.79	90.69
141	71.53	53.94	044	5.01	20.17[a]
231	30.57	30.02[a]	224	28.12	66.61
051	27.66	31.74[a]			
301	7.38	21.11[a]			
321	70.40	34.40			
251	57.59	24.86[a]			
161	45.96	41.51			

[a] Unobserved reflection

other causes). On the other hand, it has already been demonstrated that KGM crystallizes well both in fiber form and as single crystals in the mannan II form[13]. The results of the present investigation may provide an explanation for these opposing observations. Examination of the *I*222 structure has suggested that the equatorial glucose O-2 atoms can be readily accommodated in the unit cell in such a way as to facilitate hydrogen bonds with adjacent water molecules. Some short contacts, however, may arise between the glucose O-2 and O-6 atoms in neighboring chains if the O-6 remains in the *gt* position. Rotation of the latter to the *gg* position, i.e., the local formation of the O-6-*gg*-*gt* structure in regions with glucose-rich chains, eliminates these short contacts.

These possibilities resulting from the present X-ray diffraction study should be investigated further, perhaps with the single-crystal electron diffraction technique. The latter has demonstrated an ability to produce considerable structural detail[15,37–39]. The proposed hydrogen-bonding scheme, O-6 positions, and the nature of the glucose substitution in the crystal structure are some of the detail necessary to be confirmed.

ACKNOWLEDGMENTS

This work was supported by the National Science Foundation, under grants No. DMB8320548 and DMB8703725. We thank Professor T. Mizuno of the Sizuoka University for supplying a purified konjac glucomannan, and Professor William T. Winter for help with the LALS program.

REFERENCES

1 G.O. Aspinall, E.L. Hirst, E.G.V. Percival, and I.R. Williamson, *J. Chem. Soc.* (1953) 3184–3188.
2 H. Meier, *Biochim. Biophys. Acta* 28 (1958) 229–240.
3 M.L. Wolfrom, M.L. Laver, and D.L. Patin, *J. Org. Chem.* 26 (1961) 4533–4535.
4 E, Frei and R.D. Preston, *Proc. Roy. Soc. London, Ser. B*, 169 (1968) 127–145.
5 E. Frei and R.D. Preston, *Nature, London* 192 (1961) 939–943.
6 Y. Iriki and T. Miwa, *Nature, London,* 185 (1960) 178–179.
7 J. Love and E. Percival, *J. Chem. Soc.* (1964) 3345–3350.
8 R.L. Whistler and E.L. Richards, in W. Pigman and D. Horton (Eds.), (Eds.)*The Carbohydrates*, Academic Press, 1970, 2A, 447–469.
9 W. Mackie and R.D. Preston, *Planta* 79 (1968) 249–253.
10 H.D. Chanzy, A. Grosrenaud, R. Vuong, and W. Mackie, *Planta* 161 (1984) 320–329.
11 H. Bittiger and E. Husemann, *Polym. Lett.*, 10 (1972) 367–371.
12 H.D. Chanzy, M. Dube, R.H. Marchessault, and J.F. Revol, *Biopolymers*, 18 (1979) 887–898.
13 H.D. Chanzy, A. Grosrenaud, J.P. Joseleau, M. Dube, and R.H. Marchessault, *Biopolymers*, 21 (1982) 301–319.
14 I. Nieduszynski and R.H. Marchessault, *Can. J. Chem.*, 50 (1972) 2130–2138.
15 H.D. Chanzy, S. Perez, D.P. Miller, G. Paradossi, and W.T. Winter, *Macromolecules*, 20 (1987) 2407–2413.
16 K. Okuyama, S. Arnott, R.D. Preston, and M. Takayanagi, unpublished work.
17 N. Kishida, S. Okimasu, and T. Kamata, *Agr. Biol. Chem.*, 42 (1978) 1645–1650.
18 K. Kato and K. Matsuda, *Agr. Biol. Chem.*, 33 (1969) 1446–1453.
19 A. Sarko, LSQ (*Fortran least-squares curve resolution program*); SUNY College of Environmental Science and Forestry, Syracuse, NY.
20 A. Sarko, FIBRXRAY (*Fortran X-ray intensity correction program*); SUNY College of Environmental Science and Forestry, Syracuse, NY.
21 R.J. Cella, B. Lee, and R.E. Hughes, *Acta Crystallogr. Sect. A*, 26 (1970) 118–124.
22 R.E. Franklin and R.G. Gosling, *Acta Crystallogr.*, 6 (1953) 678–681.
23 S. Arnott and W.E. Scott, *J. Chem. Soc., Perkin* 2 (1972) 324–335.
24 P.J.C. Smith and S. Arnott, *Acta Crystallogr., Sect. A*, 34 (1978) 3–1.
25 P. Zugenmaier, *Biopolymers*, 13 (1974) 1127–1139.
26 W. Mackie, B. Sheldrick, D. Akrigg, and S. Perez, *Int. J. Biol. Macromol.* 8 (1986) 43–51.
27 A. Sarko and R.H. Marchessault, *J. Polym. Sci., Part C* 28 (1969) 317–331.
28 B. Sheldrick, W. Mackie, and D. Akrigg, *Carbohydr. Res.*, 132 (1984) 1–6.
29 R.H. Marchessault, M.G. Taylor, and W.T. Winter, *Can. J. Chem.* 68 (1990) 1192–1195.
30 K. Kato, T. Watanabe, and K. Matsuda, *Agr. Biol. Chem.*, 34 (1970) 532–539.
31 R. Takahashi, I. Kusakabe, S. Kusama, Y. Sakurai, K. Murakami, A. Maekawa, and T. Suzuki, *Agr. Biol. Chem.*, 48 (1984) 2943–2950.
32 H. Shimahara, H. Suzuki, N. Sugiyama, and K. Nishizawa, *Agr. Biol. Chem.*, 39 (1975) 301–312.
33 H. Shimahara, H. Suzuki, N. Sugiyama, and K. Nishizawa, *Agr. Biol. Chem.*, 39 (1975) 293–299.
34 F. Smith and C. Srivastava, *J. Am. Chem. Soc.*, 81 (1959) 1715–1718.
35 K. Kato and K. Matsuda, *Agr. Biol. Chem.*, 37 (1973) 2045–2051.
36 K. Ogawa and T. Miyanishi, unpublished work.
37 C. Guizard, H. Chanzy, and A. Sarko, *Macromolecules*, 17 (1984) 100–107.
38 E. Roche, H. Chanzy, M. Boudeulle, R.H. Marchessault, and P. Sundararajan, *Macromolecules*, 11 (1978) 86–94.
39 C. Guizard, H.D. Chanzy, and A. Sarko, *J. Mol. Biol.*, 183 (1985) 397–408.